

## Whisker formation in Sn and Pb–Sn coatings: Role of intermetallic growth, stress evolution, and plastic deformation processes

E. Chason,<sup>1,a)</sup> N. Jadhav,<sup>1</sup> W. L. Chan,<sup>2</sup> L. Reinbold,<sup>3</sup> and K. S. Kumar<sup>1</sup>

<sup>1</sup>Division of Engineering, Brown University, Providence, Rhode Island 02912, USA

<sup>2</sup>Department of Materials Science and Engineering, University of Illinois at Urbana-Champaign, Urbana, Illinois 61801, USA

<sup>3</sup>Raytheon Company IDS, Maritime Mission Center, Portsmouth, Rhode Island 02871, USA

(Received 30 January 2008; accepted 1 April 2008; published online 28 April 2008)

We have simultaneously measured the evolution of intermetallic volume, stress, and whisker density in Sn and Pb–Sn alloy layers on Cu to study the fundamental mechanisms controlling whisker formation. For pure Sn, the stress becomes increasingly compressive and then saturates, corresponding to a plastically deformed region spreading away from the growing intermetallic particles. Whisker nucleation begins after the stress saturates. Pb–Sn layers have similar intermetallic growth kinetics but the resulting stress and whisker density are much less. Measurements after sputtering demonstrate the important role of the surface oxide in inhibiting stress relaxation. © 2008 American Institute of Physics. [DOI: 10.1063/1.2912528]

Sn whiskers are widely recognized as a reliability concern when Pb-free Sn platings are used in electronics manufacturing,<sup>1,2</sup> contributing to numerous system failures.<sup>3</sup> Whiskering can be prevented by the alloying of Pb into the Sn coatings, but legislation restricting the use of Pb in manufacturing has led to their re-emergence as a problem.

Although stress in the Sn layer is accepted as a driving force for whisker formation,<sup>4–9</sup> there is a lack of understanding about how the stress is generated and how it is transmitted into the layer. Moreover, many parameters (growth process, grain size, thickness, etc.<sup>2,10–14</sup>) have been shown to play a role in whisker formation, so it is difficult to rigorously compare results from different groups. To address these issues, we have simultaneously measured the real-time evolution of whisker density, film stress, and intermetallic compound (IMC) formation on the same set of samples. These measurements allow us to observe the correlation between these parameters, e.g., how the stress saturates even though the IMC continues to grow and how whisker nucleation only occurs after the stress saturates. Our measurements point to the important role of plastic deformation in accommodating the strain induced by the IMC growth and transmitting the stress over long distances into the Sn layer. Equivalent experiments on Pb–Sn alloy layers demonstrate how the addition of Pb prevents the stress from building up during IMC growth, thus suppressing whisker formation.

The film stress was measured by using a multibeam optical system<sup>15,16</sup> to monitor the wafer curvature. For films that are thin relative to the substrate, the curvature is proportional to the sum of the stresses integrated over each layer in the film<sup>17</sup> (referred to as the force/width or stress thickness). To individually determine the average stress in the Sn or Pb–Sn layers, we measure the change in the curvature when these layers are selectively removed by etching. The volume of Cu–Sn IMC ( $\text{Cu}_6\text{Sn}_5$ ) was determined by weighing the sample before and after etching of the Sn or Pb–Sn layer (similar to the method reported by Obemdoff *et al.*<sup>18</sup> and Zhang *et al.*<sup>19</sup>). The mass difference corresponds to the

amount of Sn that has been incorporated into the IMC.

We optically monitored the whisker density by illuminating the sample at an oblique angle and measuring with a video camera over a field of view of 1 mm<sup>2</sup>. Under these conditions, the resolution is insufficient to directly image the whisker, but the light scattered from the whisker is captured as a bright spot. The technique enables a large area of surface to be monitored continuously over a long period of time and the density to be easily quantified. Results of the optical density determination were compared scanning electron microscopy (SEM) analysis of the same surface, which confirmed that the two techniques measure the same surface feature density.

The multilayer samples were fabricated on oxidized Si substrates that were coated by electron beam deposition with a 15 nm Ti adhesion layer and a 600 nm Cu layer. Pure Sn and Sn alloy layers (10 wt % Pb) were electrodeposited over the Cu from commercial plating solutions to a thickness of 1200 nm at a growth rate of 7 nm/s. A series of eight to ten samples were prepared at the same time under the same conditions; some were continuously monitored (for whisker density), while others were etched at selected time intervals to determine the IMC mass and the stress.

Measurements of the IMC volume, film stress, and whisker density from pure Sn layers electrodeposited on Cu are shown in Fig. 1 over a period of 5 days. The IMC volume [Fig. 1(a)] continuously increases with a rate that decreases for longer times. The stress in the Sn layer [Fig. 1(b)] is initially tensile but becomes increasingly compressive over time and then saturates at a value of approximately –12 MPa. The whisker density [Fig. 1(c)] remains small for an incubation period of approximately 13 h and then rapidly increases.

SEM and transmission electron microscopy (TEM) examinations show that the IMC forms by nucleation and growth of particles on the Sn side of the Cu–Sn interface (as also reported by others<sup>19–21</sup>), which is consistent with rapid diffusion of Cu into Sn.<sup>5,21</sup> These observations further show that the particles continue to grow into the Sn layer even after the IMC has formed a continuous layer at the interface.

<sup>a)</sup>Electronic mail: eric\_chason@brown.edu.

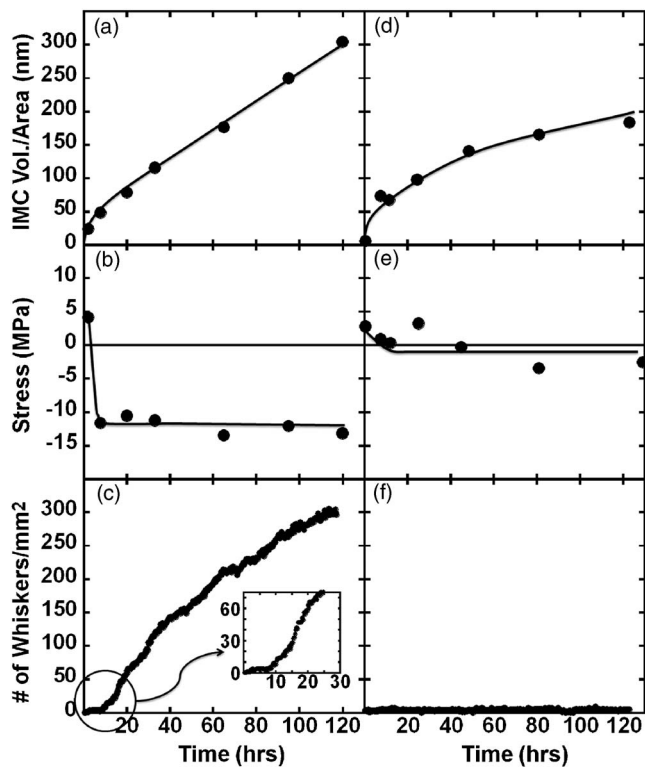


FIG. 1. Measurements of IMC volume, average stress, and whisker density in layers of [(a)–(c)] pure Sn and [(d)–(f)] Pb–Sn alloys on Cu. Drawn-in lines are guides for the eyes.

Although a relationship between IMC growth and stress generation has been previously suggested, the emphasis has been on the elastic stress fields generated around the particles<sup>4</sup> or in the layers.<sup>8,9</sup> However, the measured size of the IMC particles indicates that they grow too large for the stress to be elastically accommodated.<sup>22</sup> Therefore, plastic deformation processes in the surrounding Sn matrix must be considered, leading to the following picture for the stress evolution kinetics.

As the IMC particles grow, their volume expansion creates a stressed region that extends into the Sn layer. Large local stresses near the Sn/IMC interface cause the emission of dislocations and creation of a plastically deformed region in the vicinity of the particles. Cross-sectional TEM observations (Fig. 2) confirm the presence of numerous dislocations, both isolated and arranged in groups in the form of subgrain boundaries that result from their alignment into low energy configurations. Additionally, a flux of point defects (created by the ejection of excess Sn atoms or absorption of vacancies around the growing particles) is thought to rapidly diffuse along the grain boundaries, creating stress farther away from the interface. Spread by both dislocations and diffusional processes, the stress rises throughout the Sn layer as the IMC grows. When the stress reaches the yield stress of Sn, however, further growth of the IMC results in plastic deformation in the Sn, which does not create additional stress in the layer. Thus, a plastically deformed region eventually extends across the entire Sn layer with a uniform stress equals the Sn yield stress [ $\sim 11$  MPa (Ref. 23)]. At this point, the average stress in the layer saturates, as seen in the wafer curvature measurements. Work hardening is virtually absent at room temperature due to active dynamic recovery processes.

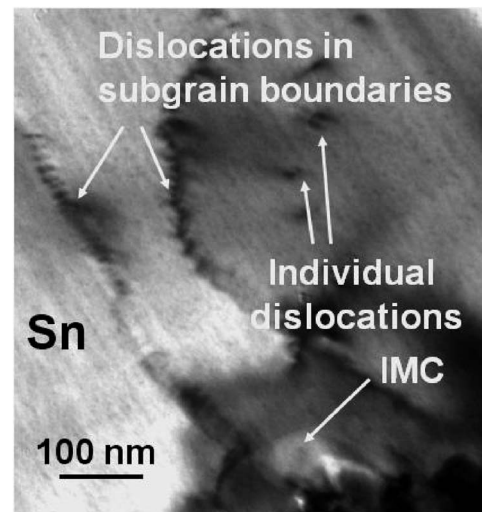


FIG. 2. Cross-sectional TEM of Sn layer on Cu showing the presence of individual dislocations and arrays of dislocations formed into subgrain boundaries.

The spreading of the stressed region across the Sn layer is instrumental for both whisker nucleation and growth. For whiskers to nucleate, the native oxide on the surface must be cracked. Elastic stress fields around growing IMC particles at the Cu–Sn interface would be too short range to induce large stresses at the surface. However, dislocation and point defect motion allow the stress to be transmitted over the entire thickness of the Sn layer and create significant stress at the Sn/oxide interface. This is reflected in the whisker density [Fig. 1(c)] which shows that the whiskers start to nucleate at the point where the stress saturates, i.e., when the stressed region has extended across the sample. After the oxide cracks, the resulting stress gradient can drive diffusional creep of atoms to the whisker base and enable growth of the whisker, as originally suggested by Tu.<sup>24</sup>

The oxide layer plays an important role in the stress development by preventing relaxation at the surface. This is shown by *in situ* measurements of the stress before and after sputtering the surface (Fig. 3). The measurements were made several days after deposition (i.e., after the stress in the Sn layer had reached saturation). The stress thickness changes

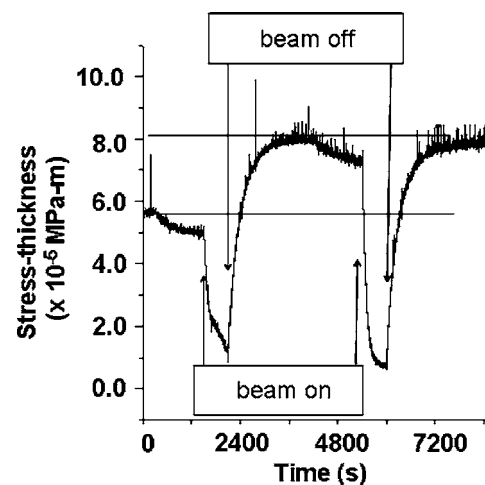


FIG. 3. Measurement of change in stress thickness in Sn on Cu layers when the surface oxide is removed by sputtering. The arrows indicate when the ion beam is turned on and off.

while the beam is turned on (arrows in figure), but when the beam is turned off, it relaxes to a more tensile value than it had before sputtering. When the process is repeated, the stress thickness after sputtering returns to the same value as before sputtering. The irreversible change after the first sequence of sputtering is due to the relaxation of stress in the Sn enabled by the removal of the oxide layer. The change in stress thickness after sputtering is the same magnitude as that caused by the compressive stress in the Sn layer. The oxide contributes to the buildup of stress in the Sn by preventing the annihilation of dislocations and point defects at the surface. When the oxide is removed, these defects are able to go to the free surface and relieve the stress. TEM observations also show that dislocations pile up below the oxidized Sn surface but are able to annihilate at clean Sn surfaces where the oxide is not present.<sup>25</sup>

To understand how the addition of Pb suppresses whiskering, equivalent measurements were performed on Sn–10%Pb alloy samples, as shown in Figs. 1(d)–1(f). The IMC growth kinetics in the alloy layer [Fig. 1(d)] are similar to pure Sn but with a slower rate at long times. However, the stress that develops in the Pb–Sn layer [Fig. 1(e)] is much less than that in the pure Sn layers [Fig. 1(b)], and the corresponding whisker density [Fig. 1(f)] does not show a measurable increase over the entire course of the experiment.

Since the average stress is different for similar amounts of IMC growth, this suggests a significant difference in the stress relaxation processes between Pb–Sn and Sn coatings. Boettinger *et al.*<sup>8</sup> have observed that the addition of Pb modifies the microstructure of Pb–Sn layers so that they have a more equiaxed grain structure than the columnar microstructure found in pure Sn. The addition of many horizontal grain boundaries may create sinks for the dislocations and point defects, which allows the strain to be accommodated without the generation of stress. Alternatively, the Pb may modify the oxide adherence or strength so that the surface can act as a sink for defects and reduce the buildup of compressive stress. At long times, the apparent reduction in the IMC growth kinetics due to Pb may also play a role in reducing stress generation. In each of these cases, the reduction in stress in the Pb–Sn layers lowers the driving force for whisker growth and/or prevents oxide cracking, which leads to a lower whisker density.

In summary, the correlations between IMC growth, stress, and whisker density highlight the mechanisms that control stress, evolution and whisker formation in Sn and Pb–Sn layers. Dislocation motion and point defect diffusion allow the stress generated around growing IMC particles to be transmitted over longer distances, saturating when the plastically deformed region spreads over the entire film thickness. The resulting stress acts as a driving force for

whisker growth, as well as a source for oxide cracking. In Pb–Sn layers, enhanced relaxation processes reduce the film stress and therefore suppress the onset of whisker formation. We note that this picture does not explain what critical stress is needed to cause whiskers to form or why the whiskers form where they do. Specific grain orientations or morphologies may also enhance the cracking of the oxide or growth of whiskers from particular grains, but such effects have not been confirmed and remain to be studied.

The authors gratefully acknowledge the support of the Brown MRSEC (DMR0079964) and EMC Corp. and helpful contributions from G. Barr, E. Buchovecky, L. B. Freund, A. Bower, and V. Shenoy.

<sup>1</sup>Recommendations on Lead-Free Finishes for Components Used in High-Reliability Products, Version 4, updated 1 December 2006, iNEMI Tin Whisker User Group (<http://www.inemi.org/cms/>).

<sup>2</sup>G. T. Galyon, *IEEE Trans. Electron. Packag. Manuf.* **28**, 94 (2005).

<sup>3</sup>For multiple examples of whisker-induced failures, see the NASA website <http://nepp.nasa.gov/whisker/>.

<sup>4</sup>B. Z. Lee and D. N. Lee, *Acta Mater.* **46**, 3701 (1998).

<sup>5</sup>K. N. Tu, *Acta Metall.* **21**, 347 (1973).

<sup>6</sup>J. Y. Song, J. Yu, and T. Y. Lee, *Scr. Mater.* **51**, 167 (2004).

<sup>7</sup>C. Xu, Y. Zhang, C. Fan, and J. A. Abys, *IEEE Trans. Electron. Packag. Manuf.* **28**, 31 (2005).

<sup>8</sup>W. J. Boettinger, C. E. Johnson, L. A. Bendersky, K.-W. Moon, M. E. Williams, and G. R. Stafford, *Acta Mater.* **53**, 5033 (2005).

<sup>9</sup>G. T. Galyon and L. Palmer, *IEEE Trans. Electron. Packag. Manuf.* **28**, 17 (2005).

<sup>10</sup>N. A. J. Sabbagh and H. J. McQueen, *Met. Finish.* **73**, 27 (1975).

<sup>11</sup>S. C. Britton, *Trans. Inst. Met. Finish.* **52**, 95 (1974).

<sup>12</sup>S. M. Arnold, Proceedings of the 43rd Annual Convention of the American Electroplaters' Society (1956), p. 26.

<sup>13</sup>R. Kawanaka, K. Fujiwara, S. Nango, and T. Hasegawa, *Jpn. J. Appl. Phys., Part 1* **22**, 917 (1983).

<sup>14</sup>T. Kakeshita, K. Shimzu, R. Kawanaka, and T. Hasegawa, *J. Mater. Sci.* **17**, 2560 (1982).

<sup>15</sup>E. Chason and J. A. Floro, *MRS Symposia Proceedings No. 428* (Materials Research Society, Pittsburgh, 1996), p. 499.

<sup>16</sup>J. A. Floro and E. Chason, *In Situ Characterization of Thin Film Growth Processes*, edited by A. Krauss and O. Auciello (Wiley, New York, 2000), pp. 191–216.

<sup>17</sup>L. B. Freund and S. Suresh, *Thin Film Materials* (Cambridge University Press, London, 2003).

<sup>18</sup>P. J. Oberndorff, M. Dittes, and L. Petit, Proceedings of the IPC/Soldertec International Conference on Lead-Free Electronics, Brussels, 2003, p. 179.

<sup>19</sup>W. Zhang, A. Egli, F. Schwager, and N. Brown, *IEEE Trans. Electron. Packag. Manuf.* **28**, 85 (2005).

<sup>20</sup>G. T. T. Sheng, C. F. Hu, W. J. Choi, K. N. Tu, Y. Y. Bong, and L. Nguyen, *J. Appl. Phys.* **92**, 64 (2002).

<sup>21</sup>K. N. Tu and R. D. Thompson, *Acta Metall.* **30**, 947 (1982).

<sup>22</sup>E. Buchovecky and A. F. Bower (unpublished).

<sup>23</sup>*Metals Handbook, Properties and Selection: Non-Ferrous Alloys and Special Purpose Materials*, 10th ed. (ASM, Metals Park, OH, 1990), Vol. 2, pp. 517–526.

<sup>24</sup>K. N. Tu, *Phys. Rev. B* **49**, 2030 (1994).

<sup>25</sup>K. S. Kumar, L. Reinbold, and E. Chason (unpublished).